

The expression of miR-30a* and miR-30e* is associated with a dualistic model for grading ovarian papillary serous carcinoma

YAN WANG¹, LV LI², ZHENYUN QU³, RUOMENG LI⁴, TIE BI⁵, JIYONG JIANG⁵ and HENAN ZHAO³

¹Laboratory Center, ²Department of Pathology, Second Affiliated Hospital of Dalian Medical University; ³Department of Pathophysiology, Dalian Medical University; ⁴Department of Anesthesiology, Second Affiliated Hospital of Dalian Medical University; ⁵Obstetrics and Gynecology Hospital, Dalian, P.R. China

Received November 25, 2013; Accepted December 27, 2013

DOI: 10.3892/ijo.2014.2359

Abstract. Histological grade has already been recognized as a very important prognostic factor for ovarian papillary serous carcinoma (OPSC). On the basis of pathogenetic mechanisms, recent findings suggest a dualistic model of OPSC consisting of types I (low-grade) and II (high-grade) cancers. High-grade OPSC is responsible for most ovarian cancer deaths. The goal of our investigation was to identify the differences in key miRNAs and possible regulators through miRNA microarray chip analysis, as well as functional target prediction and clinical outcome between the low and high-grade OPSC patients. The pathogenic basis in differentiation of ovarian cancer subtypes was studied to provide insight into diagnosis and therapy for high-grade cases. Through microarray analysis, we found that miR-30a* and miR-30e* were the top 2 significantly different miRNAs between type I and type II OPSC patients, and both were remarkably downregulated in the latter type. ATF3 and MYC were indicated as potential co-targets of miR-30a* and miR-30e*, and showed a significant upregulation in type II patients. As ATF3 and MYC are often associated with aggressive behavior and poor differentiation, especially in human cancers, these results are in good agreement with our findings and point toward a regulating differentiation function of the miR-30a* and miR-30e* genes. Further analysis using leave-one-out cross predictions and Kaplan-Meier survival analysis strongly suggested that miR-30a* and miR-30e* can be used as biomarkers to tailor histological grade before starting the regimen, and they showed important roles in ovarian cancer differentiation resulting in poorer prognosis. In general, miR-30a* and miR-30e* coupled with expression data that reveal pathogenic regulation to predict histological differentiation, may operate to direct the formation of early

detection and therapeutic approaches to individual OPSC patients, especially differentiation therapy to high-grade cases.

Introduction

Ovarian cancer (OVC) is the most lethal gynecological malignancy and ovarian papillary serous carcinoma (OPSC) is the largest histology subgroup of ovarian cancer (1-4). Growing clinical evidence suggests that histologic grade has been determined to be an important prognostic factor for ovarian serous carcinoma (5,6). Traditionally, ovarian cancer has been graded as well, moderately and poorly differentiated. But based on recent molecular genetic studies with clinical and histopathologic findings, it was proposed that OPSC tumors can be grouped into a new dualistic model based on their distinct pathogenesis (6-8). In this model, all ovarian surface epithelial tumors are divided into two groups designated type I and II. Type I tumors are mainly low-grade and have low levels of chromosomal instability. In contrast, type II tumors are generally high grade with rapidly growing, high aggressiveness and almost always have progressed to advanced stage at diagnosis, where current available therapies are seldom effective (7,9). High-grade OPSC constitutes approximately 75% of ovarian cancer but is responsible for 90% of ovarian cancer deaths (7). This has important clinical implications as evidenced by the lack of sensitivity of type II tumors to the standard cytotoxic chemotherapy that is effective for high-grade serous carcinomas (1,6,10,11). Research is urgently needed on type II tumors to better recognize the cytogenetic aberrations of this disease and design more rational approaches to early detection and targeted therapies of this type of patients.

MicroRNAs (miRNAs) are short non-coding RNA molecules of 22-24 nucleotides that play important roles by affecting various pathways related to cancer progress such as cell cycle control, apoptosis, proliferation, differentiation, metabolism and migration (12,13). As a benefit from the advances in use of miRNA microarray technologies, we can apply this approach to identify the unique miRNAs in process of diseases. Our aim was to identify the differences of key miRNAs and possible regulators through miRNA microarray chip, functional target prediction, and clinical outcome between the low and high-grade OPSC patients to find the

Correspondence to: Professor Henan Zhao, Department of Pathophysiology, Dalian Medical University, No. 9 LvShun South Road-W, Dalian 116044, P.R. China
E-mail: johnala_cn@hotmail.com

Key words: ovarian cancer, serous carcinoma, microRNA, grading, differentiation, personalized treatment

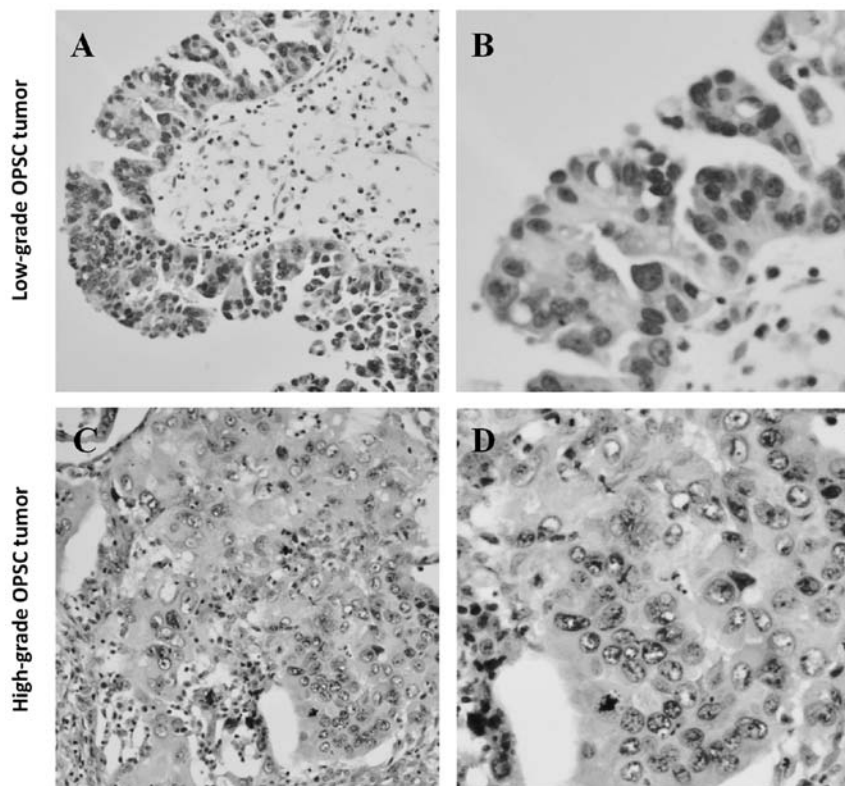


Figure 1. Examples of low-grade and high-grade ovarian papillary serous carcinomas. The diagnosis of serous carcinoma was based on criteria of the WHO classification, and the grade was assigned according to the MDACC grading system. The MDACC system is based primarily on the assessment of nuclear atypia (nuclear uniformity versus pleomorphism) in the worst area of the tumor. (A and B) Low-grade serous carcinoma is characterized as the absence of marked variation of size and shape, and the nuclei uniformly oval or round with even or slightly irregular chromatin. (C and D) Whereas, the nuclei of high-grade serous carcinoma have marked variation in size ($\geq 3:1$) and shape and a very irregular chromatin pattern. The nuclei in both low-grade and high-grade serous carcinomas may have nucleoli, and the presence of nucleoli is not a defining feature of nuclear atypia (5). Thus, uniform nuclei and visible nucleoli can be observed in most low-grade serous carcinoma, but marked nuclear pleomorphism and multinucleated cells are obvious characteristics of high-grade serous carcinoma (5).

pathogenic basis in differentiation of ovarian cancer subtypes, and to provide insight into clinical diagnosis and therapy for high-grade cases.

Materials and methods

Patient and samples. Patients, who were surgically treated for ovarian cancer at the Obstetrics and Gynecology Hospital, Dalian, China between August, 2006 and November, 2010 were identified. Corresponding 69 OPSC samples (type I=16; type II=53) that were resected at the time of primary surgery from the patients were evaluated. All pathological specimens were reviewed by two independent pathologists with no knowledge of patients' clinical data. The diagnosis of the cases was based on criteria of the International Federation of Gynecology and Obstetrics (FIGO) staging, and the grade was assigned according to the University of Texas M.D. Anderson Cancer Center (MDACC) grading system (5). The MDACC system is based primarily on the assessment of nuclear atypia (nuclear uniformity vs. pleomorphism) in the worst area of the tumor (5). Low-grade serous carcinoma is characterized as the absence of marked variation of size and shape, and their nuclei are uniformly oval or round with even or slightly irregular chromatin (Fig. 1A and B). On the contrary, the nuclei of high-grade serous carcinoma have marked variation in size ($\geq 3:1$) and shape and a very irregular

chromatin pattern (Fig. 1C and D) (5). Only serous papillary histology was included in this investigation.

miRNA microarray and data analysis. A microarray platform optimized for the analysis of a panel of 768 human miRNAs was used to analyze and compare the pattern of miRNA expression between type I (n=8) and type II (n=5) OPSC. Total RNA that was enriched for miRNAs was extracted from the FFPE tissue by using the Ambion mirVana microRNA isolation kit (Ambion, Austin, TX, USA). The quality of total RNA was assessed using the Agilent Bioanalyzer (Agilent Technologies, Santa Clara, CA, USA). Individual real-time quantitative polymerase chain reaction assays were formatted into a TaqMan low-density array (TLDA; Applied Biosystems, Foster City, CA, USA), which was performed at the Shannon McCormack Advanced Molecular Diagnostics Laboratory Research Services, Dana Farber Cancer Institute, Harvard Clinic and Translational Science Center. The normalized microarray data were managed and analyzed by Statminer version 3.0 (Integromics™, Waunakee, WI, USA).

RNA isolation and quantitative PCR. Total RNA was prepared using TRIzol reagent, following manufacturer's instructions. Quantitative Real-Time PCR (qRT-PCR) was performed using the TaqMan MicroRNA Reverse Transcription Kit (Applied Biosystems) with ABI miRNA specific primers and

Table I. PCR primers used in this study.

		Sequence (5'→3')	Calculated size of PCR primer product (bp)
ATF3	Sense	GCTAAGCAGTCGTGGTATGGG	227
	Antisense	TCCTGGAGTTGAGGCAAAGAT	
MYC	Sense	CCACCCATGGCAAATTCCATGGCA	602
	Antisense	TCTAGACGGCAGGTCAGGTCCACC	
GAPDH	Sense	TGCTGCCAAGAGGGTCAAG	1,318
	Antisense	GCCTCCAAGACGTTGTGAGT	

primer kits on an Agilent Technologies Stratagent Mx3000P (Agilent Technologies). Specific kits used were as follows: Hsa-miR-30a*: ABI#4373062; Hsa-miR-30e*: ABI#4427975. The products were detected with SYBR-Green I, and U6 small nuclear RNA as the endogenous control.

miRNA target prediction and pathway analysis. Currently, more than 900 human miRNAs are registered in the Sanger miRBase, and hundreds of potential targets are known for each miRNA. Several computational approaches were used to analyze target prediction of miRNAs, including Ingenuity Systems (Redwood City, CA, USA), MicroCosm Targets version 5 (<http://www.ebi.ac.uk/enright-srv/microcosm/htdocs/targets/v5/>), and miRBase (<http://www.mirbase.org/>). Functional analysis of these predicted targets was performed to identify biologic pathways, according to significant gene expression. In order to retrieve only the most relevant targets, and based on our previous study (4), we only listed the top 10 genes targeted by the miRNAs that showed the greatest differential expression in the patients between type I and II OPSC.

Semiquantitative reverse transcriptase PCR. The procedures for reverse transcription-polymerase chain reaction (RT-PCR) have been well established (14-16). For semiquantitative 1-step RT-PCR analysis for ATF3 and MYC, 1 µg of total RNA was used as the template in RT-PCR with the forward and reverse primers of vinculin in the kit (Takara, Dalian, China) with the following program: RT at 30°C for 10 min, 42°C for 1 h, 99°C for 5 min, and 5°C for 5 min; PCR at 94°C for 2 min, followed by 33 cycles of amplification (94°C for 1 min, 48°C for 45 sec, and 72°C for 1 min), and by extension at 72°C for 7 min. The primers for the target and housekeeping genes (GAPDH) are summarized in Table I. After amplification, the samples were separated on 2% agarose gel, visualized and quantified by Labworks-Analyst (GeneCo) software.

Immunohistochemistry (IHC). The IHC staining procedure was described previously (4). Briefly, the sections were incubated in 3% H₂O₂ for 30 min to suppress endogenous peroxidase activity after dewaxing, and then further blocked with a mixed solution [10% goat serum and 3% Albumin Bovine (BSA) in PBS] for 1 h and incubated with the primary antibodies of ATF3 (1:100 dilution; Bioworld, cat. no. BS1245); or MYC (1:100 dilution; Bioworld, cat. no. BS2261) overnight at 4°C. On the second day, these sections were incubated with streptavidin-peroxidase according to the manufacturer's instructions

Table II. Clinicopathological characteristics of the patients.

Characteristics	OPSC patients (n=69)		p-value ^b
	Type I grade ^a (n=16) No. (%)	Type II grade ^a (n=53) No. (%)	
Age at diagnosis			
Median	48.2	59.9	0.041
Range	(21-74)	(25-69)	
FIGO stage at diagnosis			<0.001 ^c
Stage II	7 (43.8)	3 (5.7)	
Stage III	8 (50.0)	37 (69.8)	
Stage IIIB	5 (31.3)	16 (30.2)	
Stage IIIC	3 (18.8)	21 (39.6)	
Stage IV	1 (6.3)	13 (24.5)	
Lymphadenectomy			
Yes	11 (68.8)	43 (81.1)	
No	4 (25.0)	8 (15.1)	
Unknown	1 (6.3)	2 (3.8)	
Median no. nodes resected	11	18	
Presence of positive nodes			<0.001
Yes	16 (20.3)	212 (65.2)	
No	52 (65.8)	103 (31.7)	
Unknown	11 (13.9)	10 (3.1)	

FIGO, International Federation of Obstetrics and Gynecology. ^aGrade according to the American Joint Committee on Cancer (AJCC) of ovarian cancer. ^bDifference between groups calculated by AVON test for age and X² test for all others. ^cFIGO stage according to early stage (stage I and II) and advanced stage (stage III and IV) in type I grade and type II grade OPSC patients.

of the staining kit (Zhongshan Goldenbridge Biotechnology Company, Beijing, China), then, 3,3'-diaminobenzidine (DAB) staining was performed. For negative controls, the conditions and the procedures were the same except that primary antibody was eliminated.

Western blot analysis. Western blot analysis was performed as previously described (14). Harvested cells were lysed in lysis buffer (Beyotime Institute of Biotechnology, Shanghai, China),

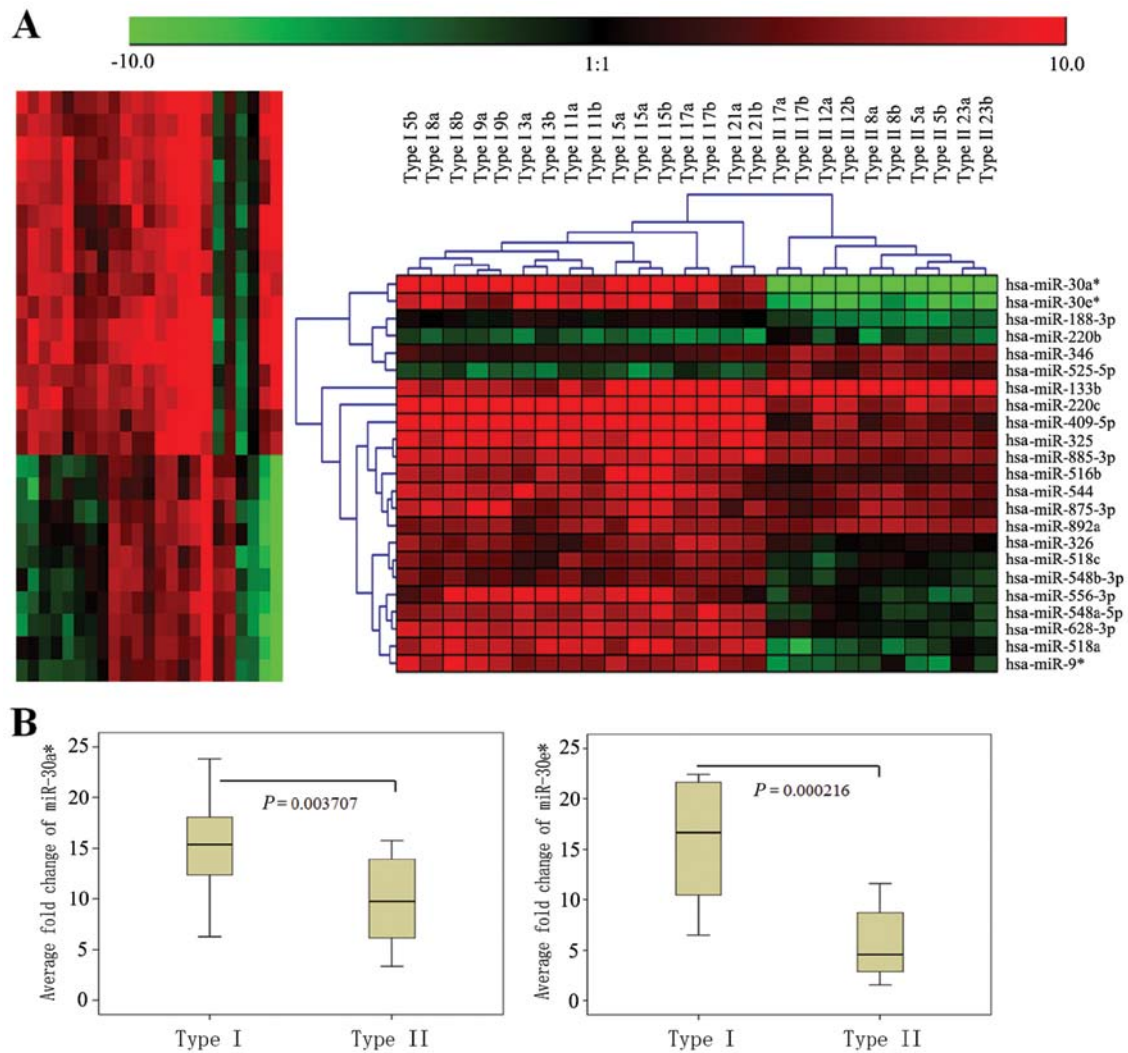


Figure 2. Results of microarray analysis and qPCR validation. (A) Unsupervised hierarchical cluster analysis of microarray assay by qRT-PCR. Among the top significantly unique miRNAs, 18 (78.3%) miRNAs are preferentially expressed in the type I samples, 5 (21.7%) miRNAs are highly expressed in the type II specimens. MiRNA-30a* and miRNA-30e* were the top 2 miRNAs that showed significantly differential expression in OPSC patients between the type I and II groups and were remarkably downregulated in the type II OPSC patients. (B) Using qRT-PCR analysis, miR-30a* and miR-30e* were found with significantly low expression in type II OPSC patients, and these results agree with microarray results. $n_{\text{miR-30a}^*}=15$ and $n_{\text{miR-30e}^*}=10$, respectively.

and the proteins (20 μg) were separated on 10% SDS-PAGE gels and transferred to nitrocellulose membranes. Membranes were blocked in PBS containing 0.05% Tween-20 (TBST) 5% non-fat milk and incubated with the following antibodies: rabbit anti-ATF3, rabbit anti-MYC and anti-GAPDH (Santa Cruz Biotechnology, Santa Cruz, CA, USA). After secondary antibody incubation, the signal analysis was performed by exposure of the blots to film, which was then scanned and band intensities were measured with Labworks-Analyst (GeneCo) software.

Statistical analysis. The results were analyzed by SPSS 17.0 (Chicago, IL, USA). Data are expressed as arithmetic means \pm SD of the number (n) of experiments. Samples were analyzed with repeated measures analysis of variance, and differences in the incidences were analyzed using ANOVA. The overall survival duration was defined as the interval (in months) between the date of initial cytoreductive surgery to date of last follow-up or death. The survival time courses

were studied using the Kaplan-Meier method, and groups were compared using the log-rank test; $p < 0.05$ was considered statistically significant.

Results

Patient characteristics. The clinicopathological characteristics of the patients who contributed to the OPSC samples are listed in Table II. Sixty-nine patients were identified to fit the study criteria, including 16 type I and 53 type II OPSC patients. The percentage of patients with advanced stage (stages III and IV) disease and the presence of positive lymph nodes were all significantly higher in patients with type II OPSC compared with patients with type I OPSC ($p < 0.001$ for all).

Analysis of microarray data. To further characterize the unique miRNAs in OPSC differentiation, specimens from the type I and type II grade OPSC patients were initially analyzed by miRNA microarray respectively. Of the 768 miRNAs

Table III. Analysis of microRNA microarray data and qRT-PCR expression of selected miRNAs.

miRNA ID	Microarray (type I vs. type II)			qRT-PCR ^a	
	- $\Delta\Delta$ Ct	p-value	Adj.p-value (q)	Type I grade	Type II grade
Upregulated miRNAs					
hsa-miR-188-3p	4.743210854	9.61E-03	4.66E-02		
hsa-miR-220c	5.720880667	7.25E-03	3.95E-02		
hsa-miR-30a*	15.862476188	3.82E-05	4.36E-03	19.29 (10.01-23.88)	7.74 (2.05-15.75)
hsa-miR-30e*	14.073272271	1.44E-05	1.06E-03	15.86 (6.48-22.42)	5.62 (1.58-11.61)
hsa-miR-325	3.030099479	2.58E-04	9.88E-03		
hsa-miR-326	1.746044354	9.25E-03	4.59E-02		
hsa-miR-409-5p	7.827316854	8.47E-03	4.33E-02		
hsa-miR-516b	2.884268854	2.95E-04	9.95E-03		
hsa-miR-518a	11.871587938	9.38E-03	4.59E-02		
hsa-miR-518c	3.82116419	9.32E-03	4.59E-02		
hsa-miR-544	2.917980104	5.31E-03	3.16E-02		
hsa-miR-548a-5p	5.114513188	4.83E-03	3.05E-02		
hsa-miR-548b-3p	4.069714854	8.38E-03	4.32E-02		
hsa-miR-556-3p	6.056558854	5.32E-04	4.36E-03		
hsa-miR-628-3p	4.913104521	5.66E-04	8.78E-03		
hsa-miR-875-3p	2.274845896	8.06E-04	5.05E-03		
hsa-miR-885-3p	3.257400396	5.23E-04	1.36E-02		
hsa-miR-9*	7.510312854	2.86E-03	2.01E-02		
Downregulated miRNAs					
hsa-miR-133b	-1.975504688	5.97E-03	3.39E-02		
hsa-miR-220b	-1.802515354	1.24E-03	1.41E-02		
hsa-miR-346	-2.917470813	8.53E-05	6.73E-03		
hsa-miR-525-5p	-4.157091438	5.18E-04	1.36E-02		
hsa-miR-892a	-2.122343771	1.57E-03	1.41E-02		

The assay found that 23 miRNAs were statistically different ($p < 0.01$) between the groups, with 18 (78.3%) miRNAs higher in the type I group and 5 miRNAs (21.7%) higher in the type II group. Three miRNAs exhibited even greater statistical significance ($p < 0.0001$ and q -value < 0.01) and of those, two were higher in the type I grade group and one was higher in the type II grade group. miR-30a* and miR-30e* were the top differential miRNAs of them (expression ratio of type I to type II = 15.86 and 14.07; $p = 3.82E-05$ and $1.44E-05$; adjust p -value = $4.36E-03$ and $1.06E-03$, respectively). ^aqRT-PCR validation only for microarray results of miR-30a* and miR-30e*. P-value and adj.p-value with boldface mean their corresponding miRNA has top obvious significance in their group.

analyzed by microarray, we found that 23 were significantly different ($p < 0.01$ for all), with at least a 2-fold ($p < 0.05$) change between type I and type II OPSC patients ($n = 8$ and $n = 5$ for the above group, respectively). The upregulation of 18 (78.3%) of these 23 key miRNAs was observed in the type I samples and 5 (21.7%) in the type II specimens (Fig. 2A and Table III). Importantly, 8 of the 18 miRNAs with distinctly statistical significance ($p < 0.001$) were lowly expressed in the type II patients. In particular, miR-30a* and miR-30e* were the top 2 miRNAs that showed significant differential expression in OPSC patients between the type I and type II groups and were remarkably downregulated in the type II OPSC patients ($p = 7.83 \times 10^{-06}$, 3.52×10^{-05} and adjusted p -value = 5.63×10^{-04} , 1.08×10^{-04} , respectively; Fig. 2A and Table III).

qPCR validation for microarray results. miR-30a* and miR-30e* were significantly downregulated in the type II OPSC when compared with the type I OPSC by using microarray analysis. In order to confirm microarray results, qRT-PCR validation was performed. RNA was isolated from

a new set of FFPE tissues to increase the likelihood that the observed differences in miRNA expression profiles represent biologically significant changes. In keeping with microarray results, miR-30a* and miR-30e* were all lowly expressed in type II grade OPSC with significance, and representative analyses are shown in Fig. 2B and Table III.

Unique miRNAs and their co-target prediction. The analysis of miRNA predicted targets was determined using several computational approaches, including Ingenuity Systems, MicroCosm Targets version 5, and miRBase. Functional analysis of these predicted gene targets can help us to identify biologic pathways with significant involvement in gene expression. In order to retrieve only the most relevant targets, we listed only genes targeted by miR-30a* and miR-30e* that were remarkably downregulated in the type II vs. type I OPSC patients, and we found they have some targets in common suggesting that they might play important roles in pathogenesis in differentiation of ovarian papillary serous carcinoma. ATF3 and MYC were indicated as potential co-targets of both miRNAs (Fig. 3A).

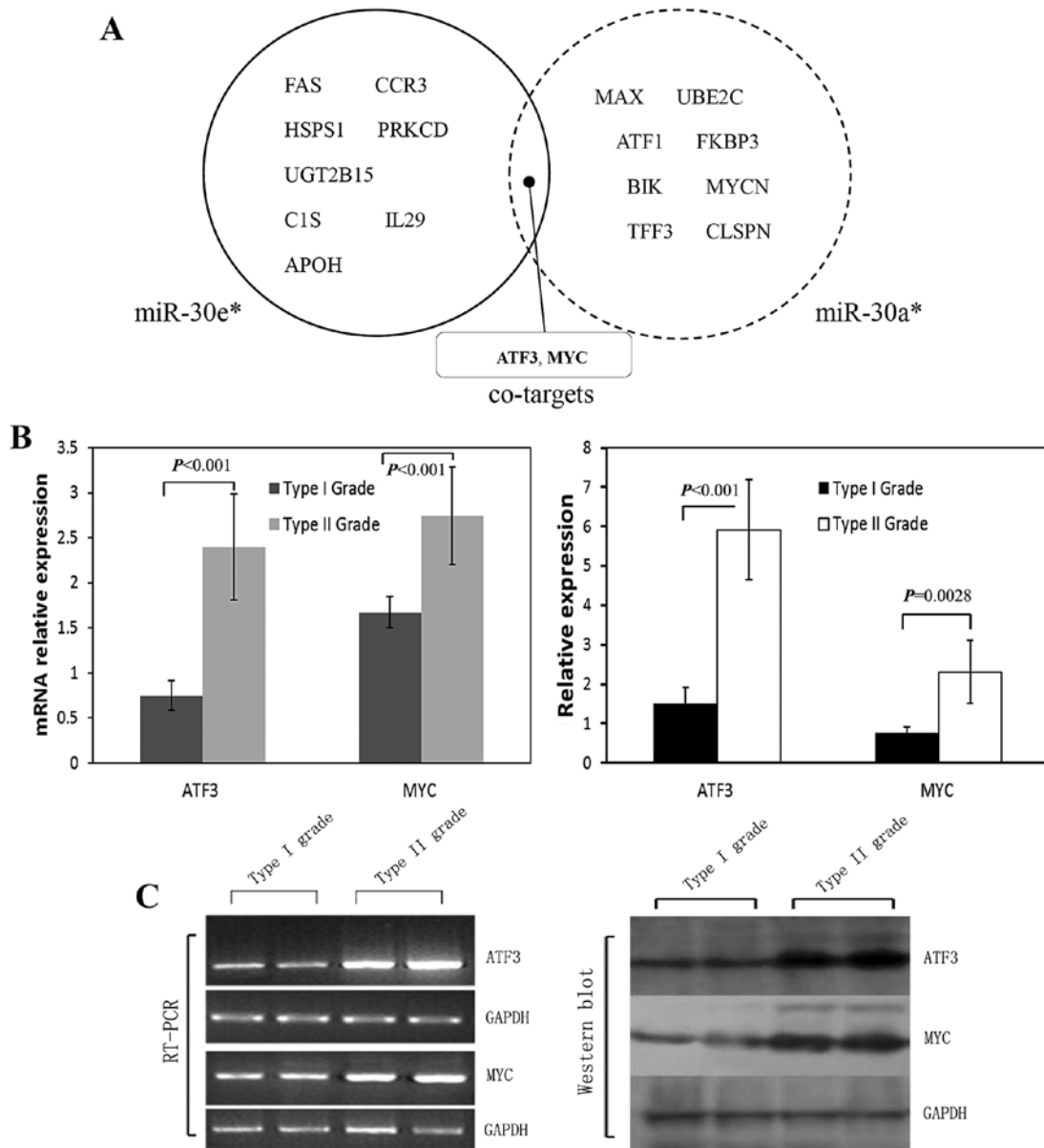


Figure 3. Target predictions and validations (RT-PCR and western blot analysis) of miRNAs through microarray analysis. (A) Venn diagram of selected miRNAs and their putative gene targets. The Ingenuity Systems, MicroCosm Targets version 5 and miRBase were used to analyze predicted targets for miR-30a* and miR-30e*. Ten top significantly unique gene targets of miR-30a* and miR-30e* are shown in Fig. 3A, respectively, and ATF3 and MYC are their co-targets. (B and C) mRNA/protein levels of ATF3 and MYC in type I and II OPSC patients were determined by RT-PCR and western blot analysis, respectively. GAPDH was used as a loading control. RT-PCR analysis for the ATF3 and MYC mRNA showed a significant upregulation in type II OPSC patients compared to type I cases ($p < 0.001$ for all; B and C). These target gene predictions were all confirmed by western blot analysis results (p -value < 0.001 and $= 0.0028$ for ATF3 and MYC, respectively; B and C).

Validation of miRNA target gene predictions. Although hundreds of targets for each miRNA were predicted using computational analysis of microarray data, the specific binding targets that directly correlated to key miRNA should be fully validated with standard approaches such as polymerase chain reaction (RT-PCR), western blot analysis or immunohistochemical assay. In target prediction analysis, ATF3 and MYC were predicted as potential co-targets of miR-30a* and miR-30e* (Fig. 3A), and present as regulators in the different pathways, which include tumorigenesis in numerous human cancers. RT-PCR analysis for ATF3 and MYC mRNA showed a significant upregulation in type II OPSC patients compared to type I cases ($p < 0.001$ for all, Fig. 3B and C). These target

gene predictions were all confirmed by western blot analysis results (p -value < 0.001 and $= 0.0028$ for ATF3 and MYC respectively, Fig. 3B and C).

Immunohistochemical assay for the ATF3 and MYC proteins showed a relevant upregulation in type II OPSC cells compared to type I OPSC cells (Fig. 4). It is clear that these co-targets were all extensively distributed in the cytoplasm of cancer cells in the tissue of type II OPSC samples comparing with the type I OPSC sections (Fig. 4A). Through analysis with Image-Pro plus vision 6.0, positive area and Integrate Optical Density (IOD) per vision-field of x400 immunohistochemistry images were detected. These results also support the conclusions of the immunohistochemical assay (Fig. 4B-C).

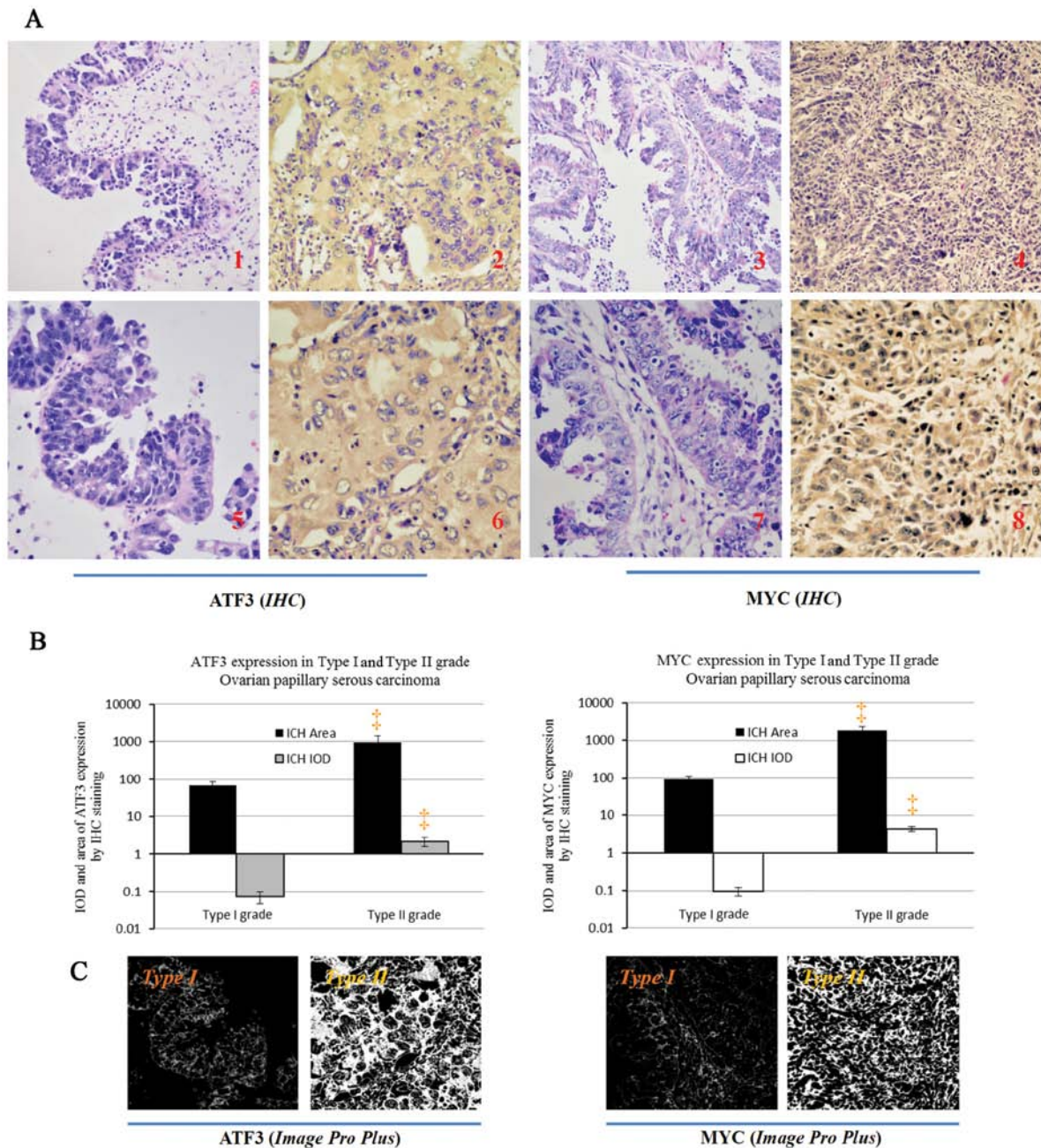


Figure 4. ATF3 and MYC protein expressions in paraffin-embedded tissues in the immunohistochemical assay of type I and type II OPSC patients. (A) Identification of the different expression of ATF3 and MYC protein between the type I grade and type II grade OPSC cells by immunohistochemistry (IHC) with counter staining of hematoxylin. ATF3 and MYC, are obviously expressed in the cytoplasm of type II grade OPSC tumor cells (A2, 4, 6 and 8) and poorly expressed in type I grade OPSC tissues (A1, 3, 5 and 7). A1, 2, 3 and 4, magnification, x200; and A5, 6, 7 and 8, magnification, x400, respectively. (B) The different expressions for positive area and integrate optical density (IOD) of ATF3 and MYC (per vision-field of x400 photograph dealt with Image-Pro plus vision 6.0) between the type I grade and type II grade OPSC tumor through immunohistochemistry staining, respectively. Images reveal (x400) the positive staining area of the above proteins with Image-Pro plus vision 6.0, respectively. Compared with the type I patients, $^{\#}p < 0.01$.

Prediction of histological grade and survival rate in OPSC patients using miR-30a and miR-30e* expression patterns.* To understand the significance of miR-30a* and miR-30e* expression patterns in epithelial ovarian cancer (EOC) differentiation, we performed a retrospective study to check the relationship between miR-30a*, miR-30e* expression and histologic grade in OPSC patients. A 50-sample training set (type I, 16; type II, 34) was used to identify miR-30a* or miR-30e* expression pattern that could predict the histological differentiation through the analysis of leave-one-out cross predictions. Using

a cutoff of 9.550466 and 11.82391 with the highest Youden's index for miR-30a* and miR-30e*, respectively, we accurately predicted the grade, and the accuracy, sensitivity and specificity are 80.0, 85.4 and 79.5% for miR-30a* and 86.0, 79.2 and 92.2% for miR-30e*, respectively (Fig. 5A and B). Mann-Whitney U tests for statistical significance ($p < 0.001$ for all groups) demonstrated the capacity of the predictor to distinguish type I OPSC patients from type II OPSC patients. The mean AUC values (area under ROC curve) of miR-30a* and miR-30e* are 0.889 and 0.895, respectively (Fig. 5C and D).

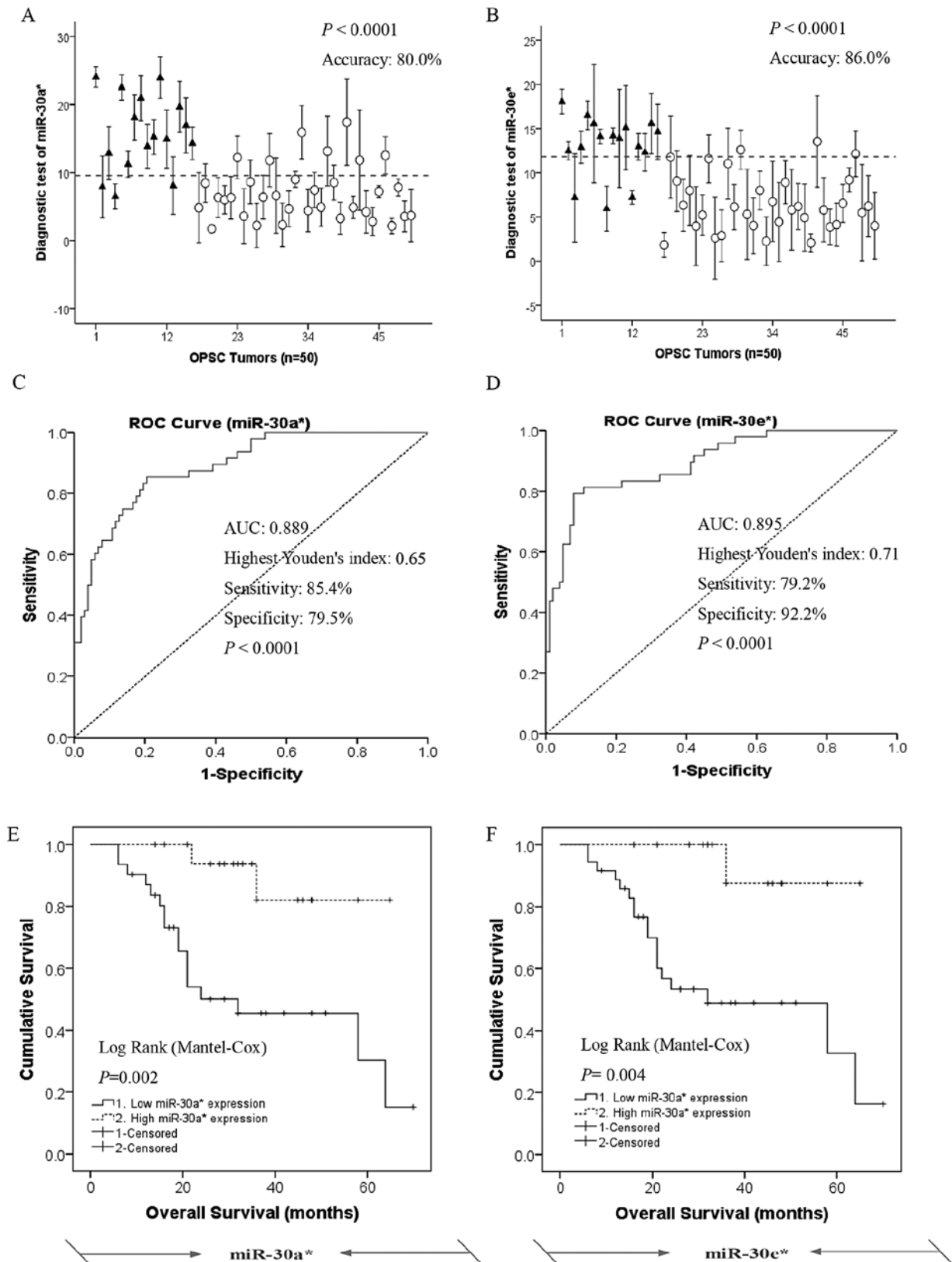


Figure 5. miR-30a* and miR-30e* serve as novel prediction and prognostic biomarkers for the grade and survival of OPSC patients. (A and B) Leave-one-out cross predictions of OPSC differentiation (black triangle, type I OPSC patients; white cycle, type II OPSC patients) with (A) miR-30a* and (B) miR-30e*, respectively, n=50 for all; cutoffs are 9.550466 and 11.82391 with the highest Youden's index for each; accuracy, sensitivity and specificity are 80.0, 85.4 and 79.5% for miR-30a* and 86.0, 79.2 and 92.2% for miR-30e*, respectively. (C and D) Receiver operating characteristic (ROC) curves of the predictions of OPSC differentiation according to (C) miR-30a* and (D) miR-30e*, respectively, n=50 for all. AUC values are 0.889 and 0.895 for miR-30a* and miR-30e*, respectively. (E and F) miR-30a* and miR-30e* serve as novel prediction and prognostic biomarkers for the response to survival of OPSC patients. The overall survival result of type I and II OPSC patients divided into two sub-sets according to high and low expression level of (E) miR-30a* and (F) miR-30e*, respectively. Diagnosis is based on the analysis of above ROC curves. Kaplan-Meier survival analysis indicated that low expression of miR-30a* and miR-30e* were all significantly associated with shorter overall survival of the OPSC patients, $p < 0.01$ for all).

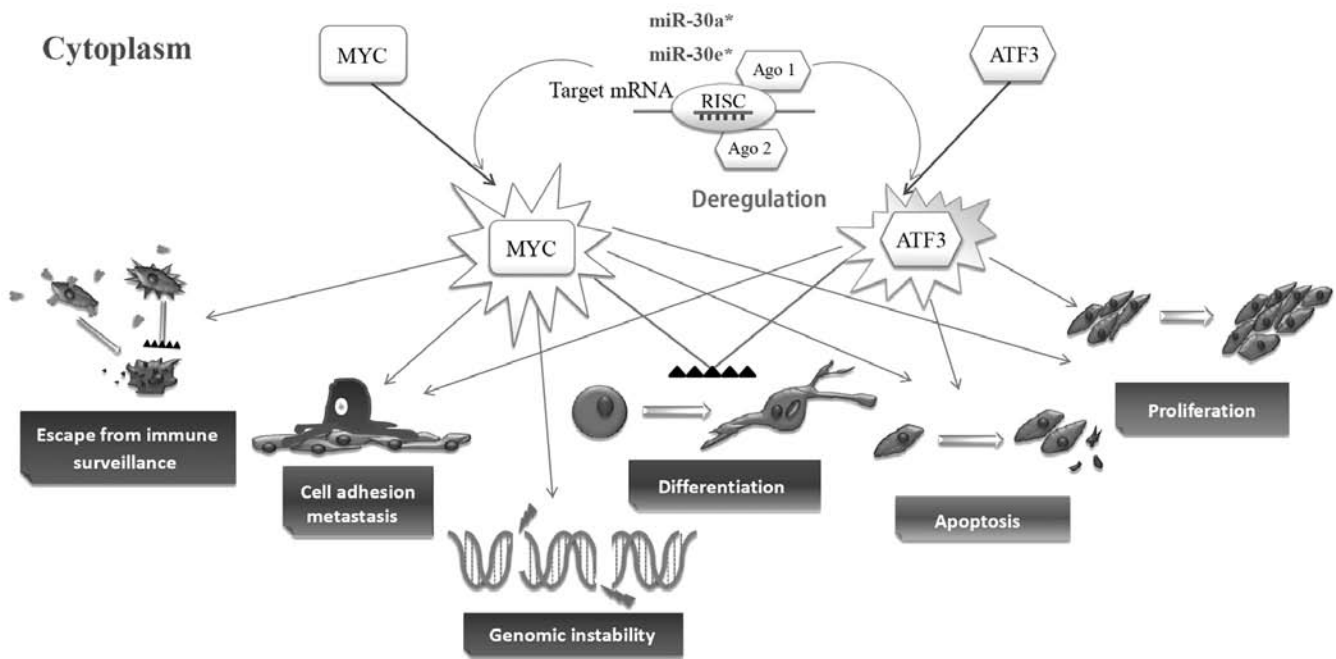


Figure 6. Cellular processes regulated by ATF3 and MYC during normal conditions and tumorigenesis. ATF3 and MYC are hallmarks of many cancers and occur as a consequence of activation of many signaling pathways that induce their expression and function as a regulator of gene transcription. As an oncogene, ATF3 contributes to the successful propagation of human cancer (4,21-24), and promote metastasis, cell adhesion and invasion, cell proliferation, apoptosis and cell differentiation (25-27). MYC is also a key regulator of many biological activities including cell growth and division, cell cycling, cell differentiation, apoptosis, and cell adhesion and motility (28). Arrows indicate promotion, and black triangle bars (▲▲▲) indicate suppression.

To further validate the predictive value of prognostic biomarkers for miR-30a* and miR-30e* expressions in clinical outcome, we performed Kaplan-Meier survival analysis for OPSC patients who were divided into two sub-sets according to high and low expression level of the miR-30a* and miR-30e* (Fig. 5E and F). Diagnosis is based on the analysis of above ROC curves. Kaplan-Meier survival analysis indicated that low expression of miR-30a* and miR-30e* was significantly associated with shorter overall survival of the OPSC patients as compared with the high miR-30a* and miR-30e* expression groups, respectively, log-rank $p < 0.01$ for all.

Taken together, these results indicate that the expression levels of miR-30a* and miR-30e* could serve as novel predictors and prognostic biomarkers for OPSC patient response to histologic grade and survival.

Discussion

Histological grade has already been recognized as a very important prognostic factor for ovarian serous carcinoma (5,6). However, there are still several unresolved issues concerning the grading of this disease in which there is no agreement regarding the designation with well, moderate, poor differentiation vs. I, II, III vs. 1,2,3,4 vs. low and high-grade (5,6). Based on the recent clinicopathological and molecular studies, some researchers proposed a model for grading serous ovarian cancer. In this model, surface epithelial tumors are divided into a two-tier system for histologic grade that is based primarily on the assessment of nuclear atypia (uniformity vs. pleomorphism) in the worst area of the tumor (1,5,7). Type I tumors are mainly low-grade and relatively genetically stable. In contrast,

high grade serous carcinoma is by far the most common type II ovarian cancer and highly aggressive. Type I tumors are associated with distinct molecular changes that are rarely found in type II tumors. Low-grade serous carcinomas typically pursue an indolent course that may last more than 20 years (1,17,18). This contrasts with conventional high-grade serous carcinoma that accounts for approximately 75% of ovarian cancer but is responsible for most of the deaths (6,19) and almost always have progressed to advanced stage at diagnosis, when current available therapies are seldom curative (7,9). Women in our study had 77% high-grade, whereas only 23% had low-grade. This is in line with the other studies examining survival of ovarian serous carcinomas using the two-tier system (6). In our investigation, we found that women with high-grade had a significantly increased risk of ovarian cancer compared with women with low-grade (Table II). Similar results were found in other studies (5,6).

Through miRNA microarray and targets prediction analysis, 23 miRNAs were found to be highly differentially expressed in tumors from type I vs. type II OPSC patients. miR-30a* and miR-30e* were the top 2 miRNAs that showed significant differential expression in OPSC patients between the type I and II, and were remarkably downregulated in the latter group, suggesting that these miRNAs are involved in differentiation of serous ovarian cancer. To further understand the mechanisms and to investigate the functions of miRNAs in the development of ovarian pathological differentiation, miRNA target prediction and pathway analysis were done. ATF3 and MYC were indicated as potential co-targets of both miRNAs, and they were validated as significantly upregulated in type II OPSC patients.

ATF3 is a member of the ATF/CREB family of transcription factors (4), as an oncogene, ATF3 contributes to the successful propagation of human cancer (4,21-24), and promotes metastasis, cell adhesion and invasion, cell proliferation, apoptosis and cell differentiation (25-27) (Fig. 6). ATF3 plays a complex role in tumor progression, and it is possible that some of the apparent contradictions in terms of the function of the ATF3 gene arise at least in part due to the difference in the cellular context (25). Similarly to ATF3, MYC levels can be activated in a wide variety of human hematological malignancies and solid tumors (28). Deregulation of MYC contributes to the genesis of a wide spectrum of human tumors through many biological activities including cell growth and division, cell cycling, cell differentiation, apoptosis and cell adhesion and motility (28) (Fig. 6). The most common MYC aberration in solid tumors is gene amplification. In ovarian cancer, MYC overexpression is observed with a frequency of around 40% (28). Importantly, MYC inactivation resulted in tumor regression and/or differentiation in several experimental systems (28-31). Jain *et al* found that even transient inactivation of MYC was sufficient to achieve tumor regression and cell differentiation (32). The above-mentioned studies revealed that ATF3 and MYC are often associated with aggressive behavior and poor differentiation, especially in human cancers (28). These results are in good agreement with our findings and point toward a regulating differentiation function of the miR-30a* and miR-30e* genes.

To further validate this hypothesis, we investigated the leave-one-out cross predictions of OPSC histological grade stratified by expression levels of miR-30a* and miR-30e*, respectively. By checking and following-up on the patient's medical records, we unexpectedly found that miR-30a* and miR-30e* can predict histological grade with accuracy of up to 80.0 and 86.0%, and AUC values are 0.889 and 0.895, respectively. Kaplan-Meier survival analysis indicated that low expression of miR-30a* and miR-30e* were all significantly associated with shorter overall survival of the OPSC patients. These findings strongly suggested that miR-30a* and miR-30e* can be used as biomarkers to tailor histological grade before starting the regimen, and they have important roles in ovarian cancer differentiation resulting in poorer prognosis.

To our knowledge, this study is the first to indicate and validate the roles and significance of miR-30a* and miR-30e* in histologic differentiation of ovarian papillary serous carcinoma. As most current cancer therapies are highly toxic and often non-specific, recently, a potentially less toxic approach, termed 'differentiation therapy', to treating this prevalent disease is raised. This approach employs agents to modify cancer cell differentiation, which on appropriate treatment, results in tumor re-programming and a concomitant loss in proliferative capacity and induction of terminal differentiation or apoptosis (33). We hope our research can improve understanding of molecular mechanisms of EOC development and progression, especially in histologic differentiation, so that we can provide improved diagnostic, prognostic and therapeutic approaches to individual patients, especially in differentiation therapy to high-grade OPSC cases.

References

1. Shih IeM and Kurman RJ: Ovarian tumorigenesis: a proposed model based on morphological and molecular genetic analysis. *Am J Pathol* 164: 1511-1518, 2004.
2. Pignata S and Vermorken JB: Ovarian cancer in the elderly. *Crit Rev Oncol Hematol* 49: 77-86, 2004.
3. Boren T, Xiong Y, Hakam A, *et al*: MicroRNAs and their target messenger RNAs associated with ovarian cancer response to chemotherapy. *Gynecol Oncol* 113: 249-255, 2009.
4. Zhao H, Ding Y, Tie B, *et al*: miRNA expression pattern associated with prognosis in elderly patients with advanced OPSC and OCC. *Int J Oncol* 43: 839-849, 2013.
5. Malpica A, Deavers MT, Tornos C, *et al*: Interobserver and intraobserver variability of a two-tier system for grading ovarian serous carcinoma. *Am J Surg Pathol* 31: 1168-1174, 2007.
6. Hannibal CG, Vang R, Junge J, Kjaerbye-Thygesen A, Kurman RJ and Kjaer SK: A binary histologic grading system for ovarian serous carcinoma is an independent prognostic factor: a population-based study of 4317 women diagnosed in Denmark 1978-2006. *Gynecol Oncol* 125: 655-660, 2012.
7. Lu D, Kuhn E, Bristow RE, *et al*: Comparison of candidate serologic markers for type I and type II ovarian cancer. *Gynecol Oncol* 122: 560-566, 2011.
8. Gloss BS and Samimi G: Epigenetic biomarkers in epithelial ovarian cancer. *Cancer Lett* 342: 257-263, 2014.
9. Kurman RJ, Visvanathan K, Roden R, Wu TC and Shih IeM: Early detection and treatment of ovarian cancer: shifting from early stage to minimal volume of disease based on a new model of carcinogenesis. *Am J Obstet Gynecol* 198: 351-356, 2008.
10. Vang R, Shih I and Kurman RJ: Ovarian low-grade and high-grade serous carcinoma: pathogenesis, clinicopathologic and molecular biologic features, and diagnostic problems. *Adv Anat Pathol* 16: 267-282, 2009.
11. Kurman RJ and Shih I: Molecular pathogenesis and extraovarian origin of epithelial ovarian cancer-shifting the paradigm. *Hum Pathol* 42: 918-931, 2011.
12. Neelakandan K, Babu P and Nair S: Emerging roles for modulation of microRNA signatures in cancer chemoprevention. *Curr Cancer Drug Targets* 12: 716-740, 2012.
13. Li C, Hashimi SM, Good DA, *et al*: Apoptosis and microRNA aberrations in cancer. *Clin Exp Pharmacol Physiol* 39: 739-746, 2012.
14. Wang Y, Wang Q, Zhao Y, *et al*: Protective effects of estrogen against reperfusion arrhythmias following severe myocardial ischemia in rats. *Circ J* 74: 634-643, 2010.
15. Li ZD, Hu XW, Wang YT and Fang J: Apigenin inhibits proliferation of ovarian cancer A2780 cells through Id1. *FEBS Lett* 583: 1999-2003, 2009.
16. Schick B, Wemmert S, Jung V, Steudel WI, Montenarh M and Urbschat S: Genetic heterogeneity of the MYC oncogene in advanced juvenile angiofibromas. *Cancer Genet Cytogenet* 164: 25-31, 2006.
17. Seidman JD and Kurman RJ: Subclassification of serous borderline tumors of the ovary into benign and malignant types. A clinicopathologic study of 65 advanced stage cases. *Am J Surg Pathol* 20: 1331-1345, 1996.
18. Smith Sehdev AE, Sehdev PS and Kurman RJ: Noninvasive and invasive micropapillary (low-grade) serous carcinoma of the ovary: a clinicopathologic analysis of 135 cases. *Am J Surg Pathol* 27: 725-736, 2003.
19. Lalwani N, Prasad SR, Vikram R, Shanbhogue AK, Huettner PC and Fasih N: Histologic, molecular, and cytogenetic features of ovarian cancers: implications for diagnosis and treatment. *Radiographics* 31: 625-646, 2011.
20. Malpica A, Deavers MT, Lu K, *et al*: Grading ovarian serous carcinoma using a two-tier system. *Am J Surg Pathol* 28: 496-504, 2004.
21. Kim MS, In SG, Park OJ, *et al*: Increased expression of activating transcription factor 3 is related to the biologic behavior of cutaneous squamous cell carcinomas. *Hum Pathol* 42: 954-959, 2011.
22. Hai T and Hartman MG: The molecular biology and nomenclature of the activating transcription factor/cAMP responsive element binding family of transcription factors: activating transcription factor proteins and homeostasis. *Gene* 273: 1-11, 2001.

23. Thompson MR, Xu D and Williams BR: ATF3 transcription factor and its emerging roles in immunity and cancer. *J Mol Med (Berl)* 87: 1053-1060, 2009.
24. Pelzer AE, Bektic J, Haag P, *et al*: The expression of transcription factor activating transcription factor 3 in the human prostate and its regulation by androgen in prostate cancer. *J Urol* 175: 1517-1522, 2006.
25. Bandyopadhyay S, Wang Y, Zhan R, *et al*: The tumor metastasis suppressor gene Drg-1 down-regulates the expression of activating transcription factor 3 in prostate cancer. *Cancer Res* 66: 11983-11990, 2006.
26. Ishiguro T, Nagawa H, Naito M and Tsuruo T: Inhibitory effect of ATF3 antisense oligonucleotide on ectopic growth of HT29 human colon cancer cells. *Jpn J Cancer Res* 91: 833-836, 2000.
27. Jang MK, Kim CH, Seong JK and Jung MH: ATF3 inhibits adipocyte differentiation of 3T3-L1 cells. *Biochem Biophys Res Commun* 421: 38-43, 2012.
28. Vita M and Henriksson M: The Myc oncoprotein as a therapeutic target for human cancer. *Semin Cancer Biol* 16: 318-330, 2006.
29. Pelengaris S, Khan M and Evan GI: Suppression of Myc-induced apoptosis in beta cells exposes multiple oncogenic properties of Myc and triggers carcinogenic progression. *Cell* 109: 321-334, 2002.
30. Shachaf CM, Kopelman AM, Arvanitis C, *et al*: MYC inactivation uncovers pluripotent differentiation and tumour dormancy in hepatocellular cancer. *Nature* 431: 1112-1117, 2004.
31. Yu D, Dews M, Park A, Tobias JW and Thomas-Tikhonenko A: Inactivation of Myc in murine two-hit B lymphomas causes dormancy with elevated levels of interleukin 10 receptor and CD20: implications for adjuvant therapies. *Cancer Res* 65: 5454-5461, 2005.
32. Jain M, Arvanitis C, Chu K, *et al*: Sustained loss of a neoplastic phenotype by brief inactivation of MYC. *Science* 297: 102-104, 2002.
33. Leszczyniecka M, Roberts T, Dent P, Grant S and Fisher PB: Differentiation therapy of human cancer: basic science and clinical applications. *Pharmacol Ther* 90: 105-156, 2001.